JOURNAL OF GEOPHYSICAL RESEARCH, VOL. 97, NO. A11, PAGES 16,971–16,979, NOVEMBER 1, 1992

Relaxation of Transient Lower Ionospheric Disturbances Caused by Lightning-Whistler-Induced Electron Precipitation Bursts

V. S. GLUKHOV AND V. P. PASKO

Department of Astronomy, Kiev State University, Vladimirskaya, Kiev, Ukraine

U. S. INAN

Space, Telecommunications and Radioscience Laboratory, Stanford University, Stanford, California

A quantitative model of the relaxation of transient lower ionospheric (D region) disturbances caused by lightning-induced electron precipitation is developed, taking advantage of known particular features of the lightning-induced disturbances, such as the fact that they are produced in typically <1 s and decay over 10-100 s. The model represents the nighttime D region as consisting of only four kinds of charged particles (electrons, positive ions, negative ions, and positive cluster ions) and is particularly suited for description of the detailed behavior of the electron density. Application of the model to some previously modeled disturbances indicates that some of the least known chemical reaction rates in the nighttime D region altitudes may be measurable using subionospheric VLF data. In the production of secondary ionization by precipitating electron bursts, the model calculations indicate the presence of a saturation effect such that the number density of the secondary electrons is not simply equal to the ion pair production rate times the burst duration. In some cases involving precipitation of $\sim$1-MeV electrons, the model predicts the formation of new layers of ionization at 50-70 km altitude that represent a different attachment-detachment quasi-equilibrium value from that of the unperturbed ambient. Such new layers may exist for up to $\sim 10^5$ s following electron precipitation bursts.

1. INTRODUCTION

Characteristic perturbations in the phase and amplitude of subionospherically propagating VLF signals have recently emerged as a powerful tool for detection and measurement of transient and localized disturbances of the lower ionosphere. Such disturbances generally occur due to a number of different physical processes, including lightning-induced electron precipitation [*Inan et al.*, 1990 and references therein] and lightning-induced heating [*Inan et al.*, 1991]. Theoretical and experimental efforts to understand these phenomena and their subionospheric VLF signatures have up to now concentrated on quantitative modeling of the wave-induced precipitation process [e.g., *Chang and Inan*, 1985; *Inan et al.*, 1989], observations of precipitating electrons on satellites and rockets [*Voss et al.*, 1984; *Goldberg et al.*, 1986], and quantitative modeling of the effect of the ionospheric disturbance on the Earth-ionosphere waveguide signal [*Tolstoy et al.*, 1986; *Poulsen et al.*, 1990; *Dowden and Adams*, 1991].

The chemical and physical relaxation processes connected with the ionospheric disturbance, on the other hand, have not yet been investigated. In the majority of works [e.g., *Inan et al.*, 1988; *Poulsen et al.*, 1990] the new state of the ionosphere (e.g., new electron density profile) immediately following the onset of the disturbance is estimated using the computed energy spectrum of precipitating electrons [*Chang and Inan*, 1985] and published ion pair production rates [*Rees*, 1963]. However, as mentioned by *Wolf and Inan* [1990], none of the existing models quantitatively addresses the time evolution of the transient ionospheric disturbances during the typically 10-100 s recovery to the ambient conditions, as exhibited by the recovery of VLF signals back to original levels. Unusually rapid recovery signatures observed at low ($L<2$) latitudes were interpreted by *Inan et al.* [1988] using an effective recombination coefficient for electrons between 50 and 150 km obtained by collecting and averaging empirical data [*Gledhill*, 1986]. While such a simple approach was found to lead to results generally consistent with data [*Inan et al.*, 1988], it does not allow the extraction of information concerning the relevant physical (or chemical) processes in the lower ionosphere.

In summary, the physical bases of the relationships between short term temporal features of phase and amplitude of the subionospheric signal and the characteristics of the lower ionosphere have not yet been studied. On the other hand, the data presented by *Gledhill* [1986] show a very broad (several orders of magnitude) distribution of recombination coefficient values, indicating a large range of possible states of the lower ionosphere and also possibly the diversity of experimental methods that were used to obtain the data. It is therefore clear that averaging over different measurements as was done by *Gledhill* [1986] oversimplifies the ionospheric conditions.

With this background, the main objective of this work is to investigate the possibility of diagnosing the state of the lower ionosphere utilizing measurements of recovery signatures in VLF signal perturbations associated with lightning discharges. In this connection, "state of the lower ionosphere" needs to be understood as, for example, the composition of charged particles, the number density distribution of different kinds of particles, and the rate coefficients for various chemical reactions between these particles.

2. PRIMARY CHEMICAL PROCESSES IN THE NIGHTTIME D REGION

Physical and chemical processes in the D region of the ionosphere are complicated and are not well understood even under relatively quiet nighttime conditions [*Chamberlain*, 1978; *Rishbeth and Garriott*, 1969; *Mitra*, 1968, 1975, 1981; *Rowe et al.*,

Paper number 92JA01596.
0148-0227/92/92JA-01596$05.00

1974]. The main reasons for our lack of knowledge in this area include the following: complicated experimental technique(s) (e.g., radars) for determination of electron density ($<10^4$ cm^{-3}) at these altitudes; the existence of numerous different kinds of negative and positive ions as well as cluster ions; the role of trace neutral components (O, O_3, NO, H_2O), the number densities of which are practically not known; and the lack of accurate knowledge of the constants of many chemical reactions between the above mentioned species. In spite of these general complications, we note that the time scales of interest for lightning-associated disturbances are of order ~100 s and that substantial simplifications of the ionospheric chemistry may be possible for the case of short (0.2–1 s) duration pulses of precipitating electrons (energies 300–1000 keV, fluxes 10^{-4}–10^{-2} erg cm^{-2} s^{-1}). Such a simplified model may be useful for extracting information about the chemical reaction constants from experimental data.

For simplicity we consider a one-dimensional model and assume that all physical quantities depend only on altitude above the Earth's surface. We neglect the processes of diffusive transport of particles and processes of wind motion (the radial wind velocity is <1 m/s, so this process can be excluded from consideration for time scales of 100 s). The main feature of the nighttime lower ionosphere is a very complicated ion chemistry due to the presence of different kinds of positive and negative ions and positive cluster ions. A review of the existing literature on this subject [*Chamberlain*, 1978; *Rishbeth and Garriott*, 1969; *Ivanov-Holodny and Nikolsky*, 1969; *Mitra*, 1968, 1975, 1981; *Rowe et al.*, 1974] leads us to conclude that a model of the D region of the ionosphere can be built which consists of only four kinds of charged particles: electrons, positive ions, negative ions, and positive cluster ions (we denote the number densities of these particles respectively as N_e, N^+, N^-, and N_x^+). Such a model would be particularly useful if we are interested only in the detailed behavior of electron density and not that of the different kinds of ions.

The positive ions (N^+) include primarily O_2^+ and NO^+ which are produced by solar Lyman α radiation (L_α) during daytime and by X rays, cosmic rays, and energetic particles at nighttime. Negative ions N^- include O_2^-, CO_3^-, NO_2^-, NO_3^-, and others. The negative ion O_2^- is produced as a result of attachment of electrons to molecular oxygen O_2 but is very quickly (~1 s) converted to other kinds of negative ions [*Chamberlain*, 1978; *Mitra*, 1975]. The detailed composition of these negative ions is not important for our purposes here. Positive cluster ions N_x^+ are all possible cluster ions which are produced from positive ions N^+ due to, for example, hydration processes with molecules of water (e.g., $H^+(H_2O)_n$) [*Chamberlain*, 1978; *Mitra*, 1975, 1981].

The primary chemical processes between the above mentioned kinds of particles are illustrated in Figure 1 and can be represented by the following kinetic equations:

$$\frac{dN_e}{dt} = I + \gamma N^- - \beta N_e - \alpha_d N_e N^+ - \alpha_d^c N_e N_x^+ \quad (1)$$

$$\frac{dN^-}{dt} = \beta N_e - \gamma N^- - \alpha_i N^- (N^+ + N_x^+) \quad (2)$$

$$\frac{dN^+}{dt} = I - BN^+ - \alpha_d N_e N^+ - \alpha_i N^- N^+ \quad (3)$$

$$\frac{dN_x^+}{dt} = -\alpha_d^c N_e N_x^+ + BN^+ - \alpha_i N^- N_x^+ \quad (4)$$

where $I = I_o + I_s(t)$, with I_o being a constant source of ionization, e.g., cosmic rays (primary production rate), for the quiet nighttime

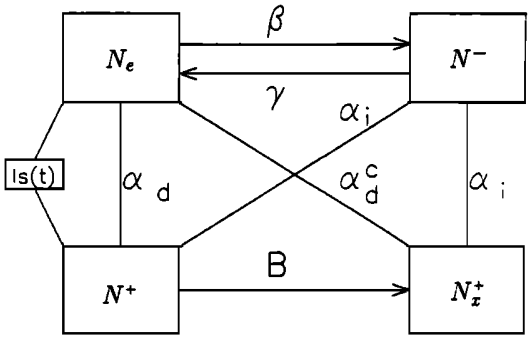

Fig. 1. Schematics of a model of the nighttime D region consisting of four different charged particles and interactions between these particles considered in this work.

D region and $I_s(t)$ being the source of ionization due to electron precipitation. The effective electron attachment rate β is given as [*Rowe et al.*, 1974]

$$\beta = 10^{-31} N_{O_2} N_{N_2} + 1.4 \times 10^{29} \left(\frac{300}{T}\right) e^{-\frac{600}{T}} N_{O_2}^2 \quad \text{s}^{-1}$$

where N_{O_2} and N_{N_2} are number densities of molecular oxygen and nitrogen, and T is the temperature of electrons (for the nighttime D region we assume T=200° K). Dependence of β on altitude is illustrated in Figure 2 by a solid line.

The value of the effective electron detachment rate γ is not well known (see comments by *Mitra* [1975]). One possible approximation for this quantity is $\gamma \simeq 3 \times 10^{-17} N$ s^{-1} [*Ivanov-Holodny and Nikolsky*, 1969], where N is total density of neutrals. This expression gives values consistent with those plotted by *Mitra* [1975]. Note that this γ includes both γ_1 and γ_2 as discussed by *Mitra* [1975]. We believe that application of the model discussed in this work to data could potentially allow better estimation of the quantity γ. The height variation of γ (due simply to the height variation of N) is illustrated in Figure 2 by a long-dashed line.

The effective coefficient of dissociative recombination α_d has values in the range 10^{-7} to 3×10^{-7} cm^3 s^{-1} [*Chamberlain*,

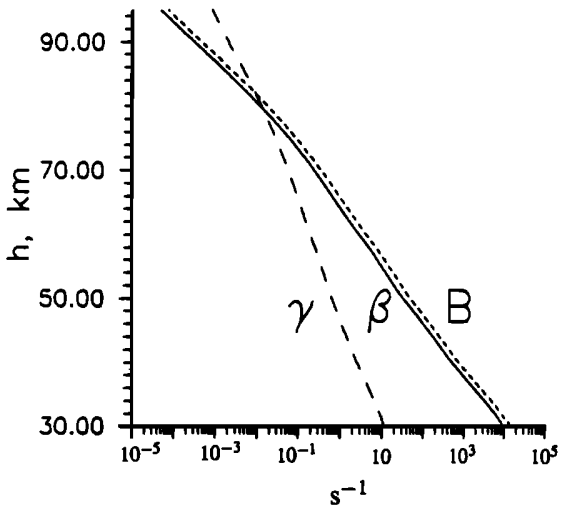

Fig. 2. Variations with altitude of attachment coefficient β, detachment coefficient γ, and coefficient of conversion of positive ions into positive cluster ions B.

1978; *Mitra*, 1968; *Rowe et al.*, 1974], whereas the effective coefficient of recombination of electrons with positive cluster ions α_d^c is not well known but lies in the range $\sim 10^{-5}$ to 10^{-6} cm^3 s^{-1} [*Rowe et al.*, 1974]. In our calculations below, we assume the same value as did *Mitra* [1975], i.e., $\alpha_d^c = 10^{-5}$cm^3 s^{-1}. The typical value of the effective coefficient of ion-ion recombination α_i (mutual neutralization) for all kinds of positive ions with negative ions is $\sim 10^{-7}$ cm^3 s^{-1} [*Mitra*, 1968; *Rowe et al.*, 1974].

The effective rate of conversion of positive ions into positive cluster ions, B [e.g., *Rowe et al.*, 1974; *Mitra*, 1975], has a typical value of $B=10^{-31}N^2$ s^{-1} where N is the total density of neutrals. The variation of the quantity B with altitude is illustrated in Figure 2 by a short-dashed line.

With the unperturbed distributions of electrons and three kinds of ions for the quiet nighttime D region being defined as above, and using equations (1)-(4), we can completely describe the processes of formation as well as relaxation of transient disturbances of the lower ionosphere as long as the source function $I_s(t)$ is known. The source function $I_s(t)$ can in turn be estimated from the precipitated flux using the ion pair production rates given by *Rees* [1963] so that the new distributions of electrons and positive ions caused by the precipitation can be evaluated.

The ambient (unperturbed) distribution of electrons N_{oe} is chosen to be the same as that used in previous papers [*Reagan et al.*, 1981; *Inan et al.*, 1988; *Poulsen et al.*, 1990]. This distribution is illustrated in Figures 4*a*, 5*a*, and 6*a* at time t=0. The unperturbed number density of negative ions, N_o^-, equals λN_{oe}, where λ is represented in Figure 3 (taken from *Rishbeth and Garriott* [1969, p. 111]), reasonably consistent with results of *Mitra* [1975] which indicate that $\lambda \simeq 1$ at 78-80 km at night. The relative composition of negative ions, λ, is not an accurately known parameter, and its value can be less than that represented in Figure 3 [*Chamberlain*, 1978]. At the same time, the results obtained below are not critically dependent on this parameter. N_o^- is represented in Figures 4*b*, 5*b*, and 6*b* at time t=0. Unperturbed distributions of positive ions (N_o^+) are represented in Figures 4*c*, 5*c*, and 6*c*, and unperturbed distributions of positive cluster ions are represented in Figures 4*d*, 5*d*, and 6*d* [*Danilov et al.*, 1981; *Rowe et al.*, 1974]. This is also consistent with *Mitra* [1975], who pointed out that the level at which the clusters begin to disappear was ~86 km at night. We assume that the condition of charge neutrality is satisfied at all times:

$$N_{oe} + N_o^- = N_{ox}^+ + N_o^+ \tag{5}$$

It should be noted that under quiet nighttime conditions in the D region of the ionosphere the main positive ions at altitudes <85 km are positive cluster ions (N_{ox}^+).

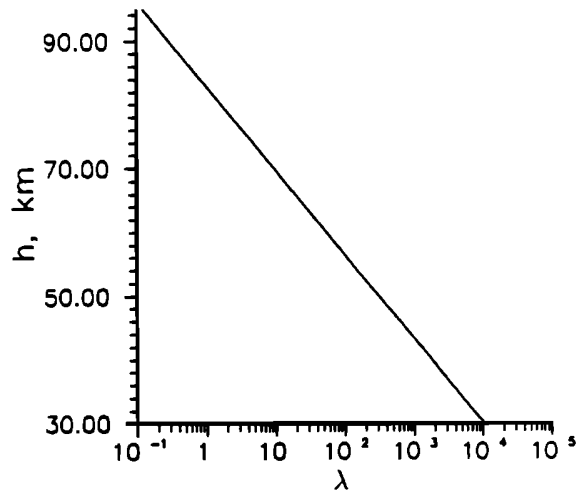

Fig. 3. Variation with altitude of the relative composition of negative ions $\lambda = N_o^-/N_{oe}$.

3. Description of the Model

In this section we describe our model and examine the system behavior in selected parameter regimes.

3.1. General Formulation

Let us assume that the unperturbed (i.e., ambient) distribution of particles as defined in the previous section is due to some external steady source I_o. The equilibrium conditions (i.e., $d/dt = 0$) can then be written as

$$I_o + \gamma N_o^- - \beta N_{oe} - \alpha_d N_{oe} N_o^+ - \alpha_d^c N_{oe} N_{ox}^+ = 0 \tag{6}$$

$$\beta N_{oe} - \gamma N_o^- - \alpha_i N_o^- (N_o^+ + N_{ox}^+) = 0 \tag{7}$$

$$I_o - B N_o^+ - \alpha_d N_{oe} N_o^+ - \alpha_i N_o^- N_o^+ = 0 \tag{8}$$

$$-\alpha_d^c N_{eo} N_{ox}^+ + B N_o^+ - \alpha_i N_o^- N_{ox}^+ = 0 \tag{9}$$

We further assume that during some period of time τ_s, new electrons N_e and new positive ions N^+ (N^+=N_e) are injected into the system. Such a process can be described by some source function $I_s(t)$ (the ionization rate per unit volume). To simplify analysis we define $I_s(t)$ as

$$\begin{aligned} I_s(t) &= I_s = \text{const}, \qquad 0 < t < \tau_s \\ I_s(t) &= 0, \qquad t > \tau_s, t < 0 \end{aligned} \tag{10}$$

The dependence of $I_s(t)$ on altitude above the Earth surface can be calculated in the same way as was done by *Rees* [1963]:

$$I_s = F \frac{(\xi_o/\tau_o)}{\Delta\xi_{\text{ion}}} \lambda' \left[\frac{z}{R}\right] \frac{n_\mu(z)}{n_\mu(R)} \tag{11}$$

where F is the flux of precipitated particles in units of cm^{-2} s^{-1}; ξ_o is average initial energy of particles in eV; $\Delta\xi_{\text{ion}}$ is effective energy for production of one electron-ion pair (~35 eV is adopted as a typical value); $\tau_o = R/\rho$, where ρ is the mass density in units of g/cm^2 at depth R, where R is the lowest depth of penetration in units of g/cm^2 and is defined as $R = 4.57 \times 10^{-6}\xi_o^{1.75}$($\xi_o$ here is in units of keV); z is the depth of atmosphere in units of g/cm^2; z/R is the fractional depth of penetration into the atmosphere, and $\lambda'(z/R)$ is the fractional energy dissipation (i.e., the distribution function of energy dissipation as tabulated by *Rees* [1963]); $n_\mu(z)$ and $n_\mu(R)$ are the number densities of ionizable atoms or molecules at atmospheric depth z and R respectively.

To calculate I_s from (11) we need to know the relationship between atmospheric depth z and altitude h above the surface of Earth and the mass and number density of neutrals. This information for altitudes >60 km was taken from Table 1 of *Rees* [1963]. For altitudes <60 km we used the U.S. Standard Atmosphere table as given by *Chamberlain* [1961]. Linear interpolation was used to obtain parameter values for altitudes not listed in these tables.

The electrons produced by ionization, as a rule, have energies of several eV while the processes considered below involve only thermal electrons (<1 eV). Therefore, some time period of electron thermalization must exist. It is clear that this time decreases

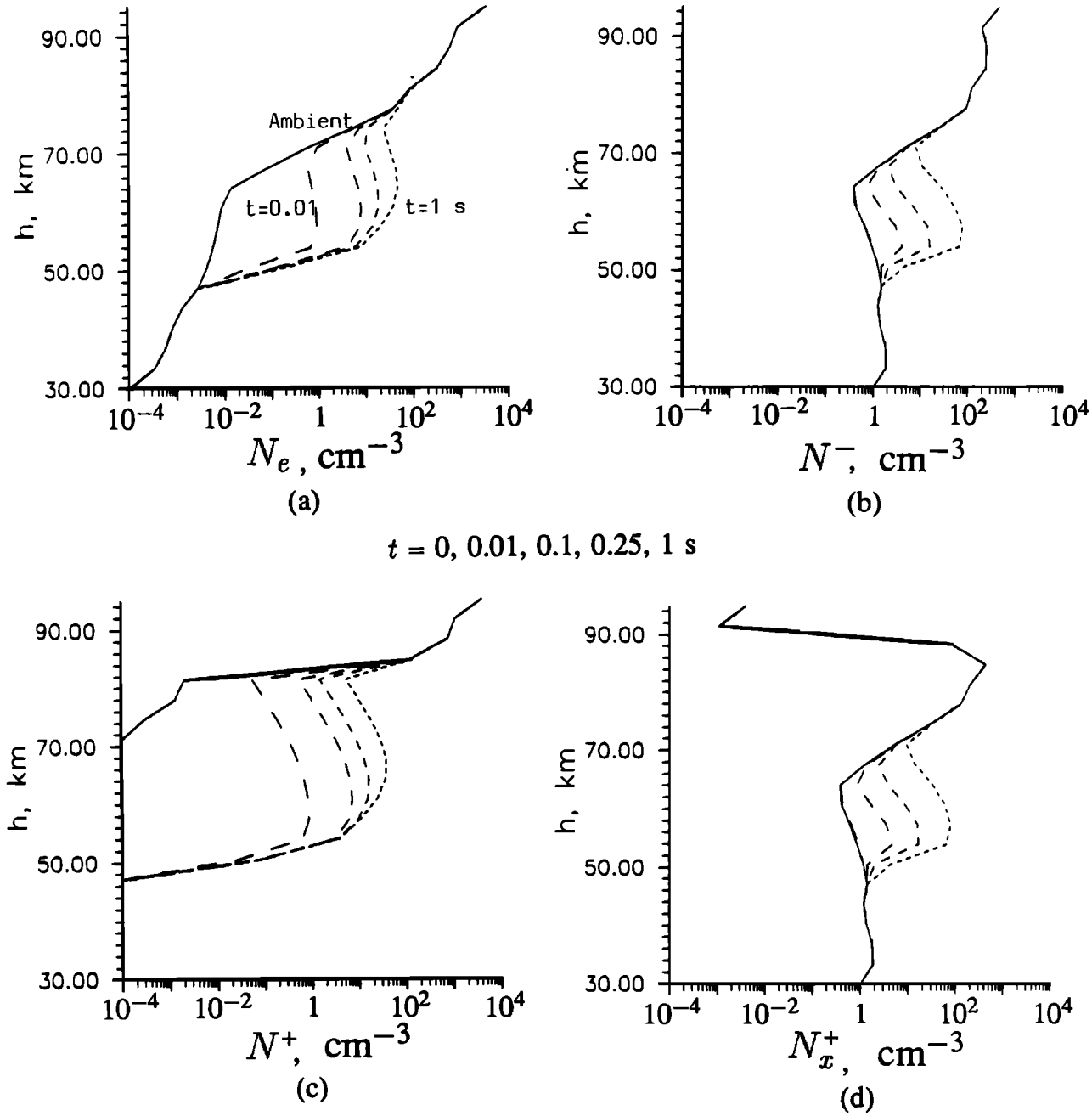

Fig. 4. Time evolution of the density of different charged particles (a) electrons, (b) negative ions, (c) positive ions, (d) positive clusters) as a function of altitude during a short electron precipitation burst. Results were obtained for the following parameters of precipitated particles: flux=10^{-2} erg cm^{-2} s^{-1}, energy E=1 MeV, and duration of electron burst τ_s=1 s. Different curves correspond to times t= 0, 0.01, 0.1, 0.25, and 1 s during the perturbation. Solid lines correspond to quiet night conditions (t= 0 s). Length of dashes decreases with increasing time. Note that curves for times t=0 s and t= 0.01 s practically coincide in the case of N^- (Figure 4*b*) and N_x^+ (Figure 4*d*).

with increasing number density of neutrals. Estimates given by *Chamberlain* [1961] suggest that for altitudes <200 km the thermalization time is $\ll$1 s. Taking into account also the exponential increase in the number density of neutrals with decreasing altitude, it appears that the electron thermalization time is very small in comparison with the time scale of interest in this work. For our purposes, we assume that secondary electrons immediately become thermalized and are available to take part in all the chemical reactions described above.

In equations (1)-(4) we replace N_e with $N_{oe}+N_e(t)$, N^+ with $N_o^+ + N^+(t)$, N^- with $N_o^- + N^-(t)$, and N_x^+ with $N_{ox}^+ + N_x^+(t)$, and combine with equations (6)-(9) to obtain

$$\frac{dN_e}{dt} = I_s + \gamma N^- - \beta N_e - \alpha_d(N_{oe}N^+ + N_e N_o^+ + N_e N^+) - \alpha_d^c(N_{oe}N_x^+ + N_e N_{ox}^+ + N_e N_x^+) \quad (12)$$

$$\frac{dN^-}{dt} = \beta N_e - \gamma N^- - \alpha_i[N_o^-(N^+ + N_x^+) + N^-(N_o^+ + N^+ + N_{ox}^+ + N_x^+)] \quad (13)$$

$$\frac{dN^+}{dt} = I_s - BN^+ - \alpha_d(N_{oe}N^+ + N_e N_o^+ + N_e N^+) - \alpha_i(N_o^- N^+ + N^- N_o^+ + N^- N^+) \quad (14)$$

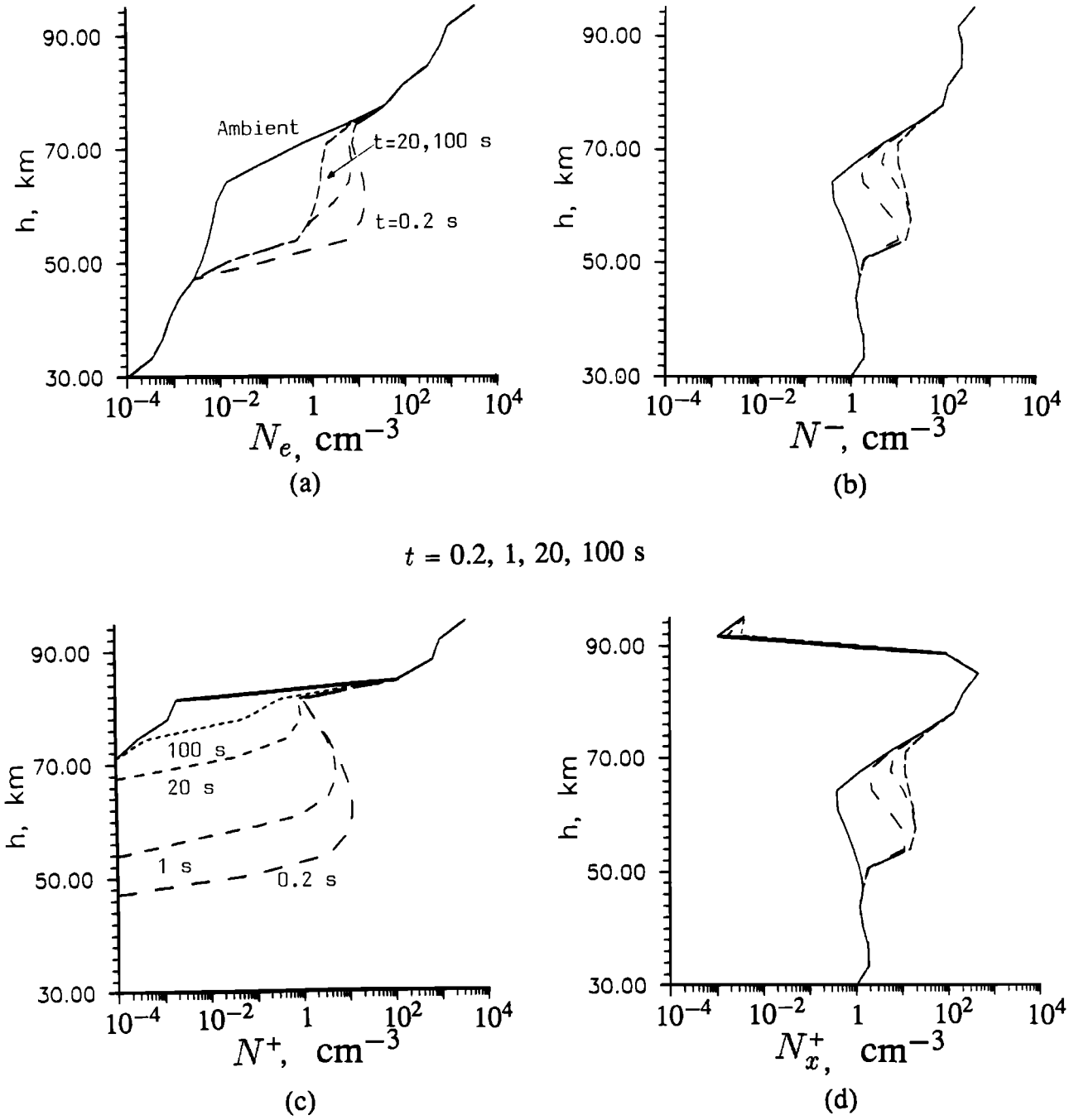

Fig. 5. Results of the simulation of the relaxation of an ionospheric disturbance produced by a precipitating electron burst of duration 0.2-s and energy flux of 10^{-2} erg cm^{-2} s^{-1}, respectively, consisting of 1- MeV electrons. Different curves represent snapshots of the relaxation process at t= 0.2, 1, 20, and 100 s. Again, length of dashes decreases with increasing time, and the solid lines are the quiet night distributions (at t= 0 s). Note that curves which correspond to N_e (Figure 5*a*), N^- (Figure 5*b*) and N_x^+ (Figure 5*d*) coincide for times t= 20 and 100 s.

$$\frac{dN_x^+}{dt} = -\alpha_d^c(N_{oe}N_x^+ + N_eN_{ox}^+ + N_eN_x^+) + BN^+ - \alpha_i(N_o^-N_x^+ + N^-N_{ox}^+ + N^-N_x^+) \quad (15)$$

Any one of the above four equations can be derived from the other three using the charge neutrality condition:

$$N_x^+ + N^+ = N_e + N^- \quad (16)$$

3.2. Approximate Solution for $0 < t < \tau_s$: Formation of the Disturbance

In the general case the system of equations (12)-(15) can be solved only by numerical methods. However, upon close examination we see that the different terms on the right hand side of equations (12)-(15) have very different magnitudes. Our estimates indicate that at altitudes of precipitation of particles with energies 300–1000 keV (~60–80 km) the terms describing the attachment-detachment processes (with rates β and γ) and conversion of positive ions to positive cluster ions (with rate B) are dominant. Having neglected all other terms, one can rewrite the system of equations (12)-(15) in the form

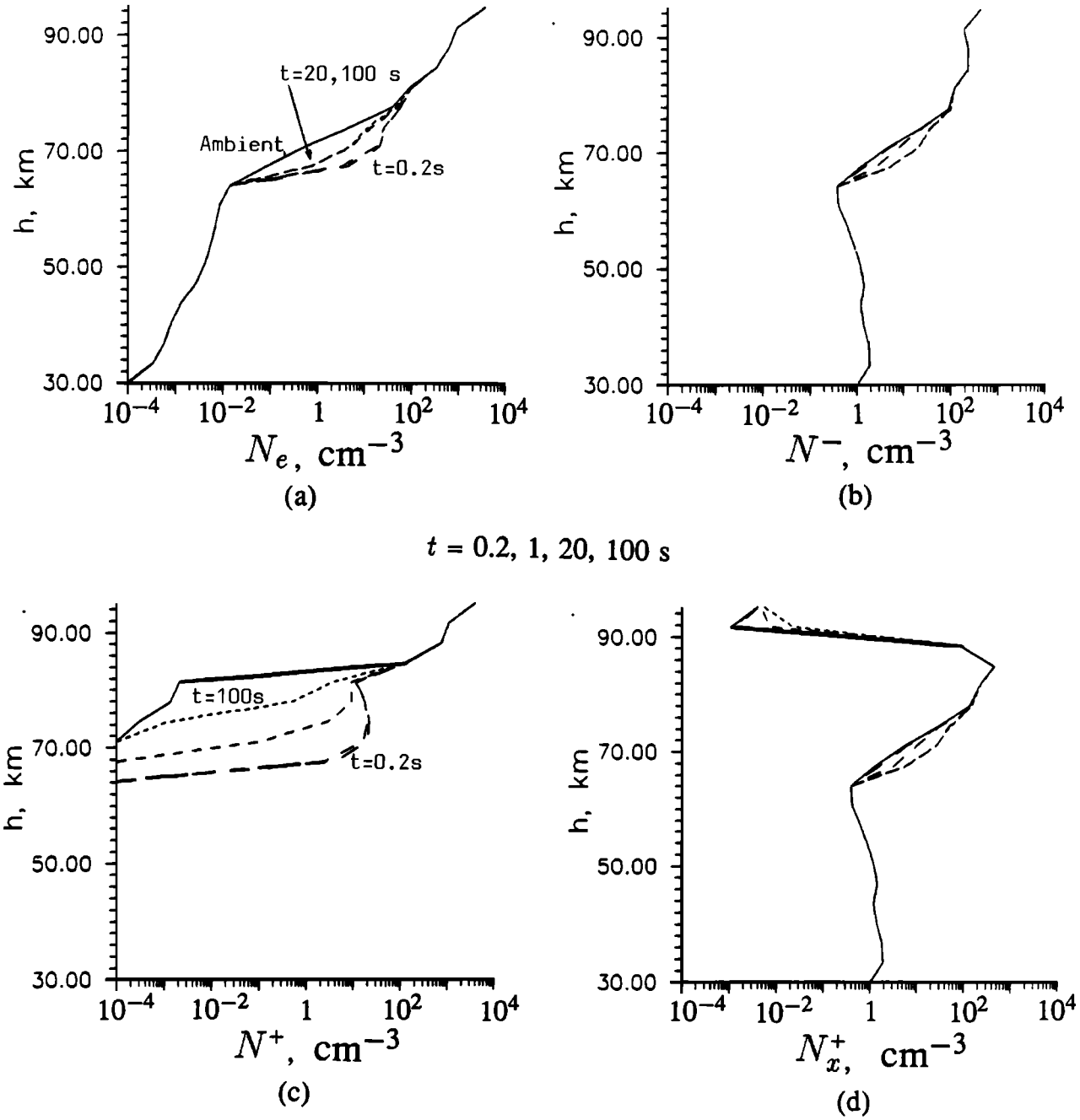

Fig. 6. Same as Figure 5 but for precipitating electrons of 300-keV energy.

$$\frac{dN_e}{dt} = I_s(t) + \gamma N^- - \beta N_e \tag{17}$$

$$\frac{dN^-}{dt} = \beta N_e - \gamma N^- \tag{18}$$

$$\frac{dN^+}{dt} = I_s(t) - BN^+ \tag{19}$$

$$\frac{dN_x^+}{dt} = BN^+ \tag{20}$$

The solution of this system for $0< t < \tau_s$ with initial conditions $N_e=N^-=N^+=N_x^+=0$ at $t=0$ and taking into account (10) can be written as

$$N_e = \frac{\gamma I_s t}{\gamma+\beta} + \frac{I_s\beta}{(\gamma+\beta)^2}\left[1 - e^{-(\gamma+\beta)t}\right] \tag{21}$$

$$N^- = I_s t - N_e \tag{22}$$

$$N^+ = \frac{I_s}{B}(1 - e^{-Bt}) \tag{23}$$

$$N_x^+ = I_s t - N_+ \tag{24}$$

and for $t > \tau_s$ we have

$$N_e = \frac{\gamma I_s \tau_s}{\gamma+\beta} + \frac{I_s \beta}{(\gamma+\beta)^2} e^{-(\gamma+\beta)(t-\tau_s)} \left[1 - e^{-(\gamma+\beta)\tau_s}\right] \tag{25}$$

$$N^- = I_s \tau_s - N_e \tag{26}$$

$$N^+ = \frac{I_s}{B}\left[1 - e^{-B\tau_s}\right] e^{-B(t-\tau_s)} \tag{27}$$

$$N_x^+ = I_s \tau_s - N^+ \tag{28}$$

We can now consider some simple limiting cases. From (21) for $t \to 0$ or $(\gamma+\beta)t \ll 1$ we have

$$N_e = I_s t \tag{29}$$

This result simply indicates that, because we consider small time scales, the attachment-detachment processes have not yet developed. If $(\gamma+\beta)t \gg 1$ and $\beta \gg \gamma$ (for example, at ~55 km altitude: $\beta \simeq 10\ s^{-1}$, $\gamma \simeq 0.4\ s^{-1}$) one can obtain

$$N_e \simeq \frac{\gamma}{\beta} I_s t + \frac{I_s}{\beta} \tag{30}$$

From (29), and (30) we note that a steady source I_s of ionization applied for a time of τ_s does not lead to an electron density enhancement of $I_s\tau_s$. Indeed, for times $t < \tau_s$, when the condition $(\gamma+\beta)t \ll 1$ is not satisfied, we note that electron density enhancement is reduced by a factor of γ/β. This result represents a significant correction to previous estimates (e.g., by *Inan and Carpenter* [1987] and *Inan et al.* [1988]) of maximum electron density produced by precipitating electron bursts which were simply based on the product of the ion pair production rate and the pulse duration. Manifestations of this "saturation" effect in a particular example are illustrated below in section 4.

3.3. *Approximate Solution for $\tau > \tau_s$: Relaxation of the Disturbance*

If we again consider solution (25) and assume that $(\gamma+\beta)t \gg 1$ and $t \gg \tau_s$ then we have

$$N_e = \frac{\gamma I_s \tau_s}{\gamma+\beta} \neq 0 \tag{31}$$

indicating that under our assumptions (neglecting recombination processes) the perturbation of electron number density does not disappear even after a long time and acquires a new attachment-detachment equilibrium value. This result can possibly be used to determine $\gamma/(\gamma+\beta)$ using experimental data on phase perturbations of VLF subionospheric waves. The temporal recovery signatures in such cases may exhibit relaxation to a new constant level rather than the typically observed recovery to prior signal levels or the projected levels.

It should be noted that for typical values of τ_s ~0.2 s at altitudes ≥60 km we have $(\gamma+\beta)\tau_s \ll 1$ and $N_e(\tau_s) = I_s\tau_s$. For $t \to \infty$ the number density of electrons is given by expression (31). It is interesting that for altitudes ~80 km we have $\gamma \simeq \beta \simeq 10^{-2}\ s^{-1}$ (see Figure 2) and for $t \to \infty$ and by using (31) we can obtain $N_e(\tau_s) \simeq N_e(\infty)$. Thus, one can see that attachment-detachment processes play an insignificant role in the evolution of the electron number density at these altitudes.

The above analysis can be summarized as follows. The quasi-equilibrium distribution of electron number density (31) is achieved in a time period of $t_o \leq 10$ s (~60 km), and/or $t_o \leq 1000$ s (~80 km). For typical values of B (see Figure 2) we have $Bt_o \gg 1$ and the following expressions for number densities of different kinds of particles can be obtained:

$$N_e(t_o) \simeq \frac{\gamma I_s \tau_s}{\gamma+\beta} \tag{32}$$

$$N^-(t_o) \simeq \frac{\beta}{\gamma} N_e(t_o) \tag{33}$$

$$N^+(t_o) \simeq 0 \tag{34}$$

$$N_x^+(t_o) \simeq I_s \tau_s \tag{35}$$

The attachment-detachment processes we mentioned above are the fastest in the system under consideration. It can be seen from the system of equations (12)-(15) that the second significant process in our system is the dissociative recombination of electrons with positive cluster ions (note that $\alpha_d^c \gg \alpha_d$). Moreover, for altitudes ≥80 km this process has a rate close to that of attachment-detachment, due primarily to the rapidly increasing number density of positive cluster ions with altitude (N_{ox}^+ may be as large as $10^3\ cm^{-3}$). Since for altitudes <~80 km attachment-detachment processes are still rapid, a second-order approximation in our system can be expressed as a solution of the equation

$$\frac{dN_e}{dt} = -\alpha_d^c (N_{oe} N_x^+ + N_e N_{ox}^+ + N_e N_x^+) \tag{36}$$

We further assume that

$$N^- = \frac{\beta}{\gamma} N_e, \qquad N_x^+ = N_e\left(\frac{\gamma+\beta}{\gamma}\right)$$

with initial conditions (32)-(35), in other words that N^- and N_x^+ adiabatically follow N_e. Note that equation (36) is only approximately true for altitudes ≥80 km. The solution of (36) can be written in the form

$$N_e = -\frac{A}{2}\left[1 - \frac{1 + \tanh((t-t_o)/\tau_c) + 2\gamma I_s \tau_s/(\gamma+\beta)A}{1 + (1 + 2\gamma I_s \tau_s/(\gamma+\beta)A)\tanh((t-t_o)/\tau_c)}\right] \tag{37}$$

where

$$A = N_{oe} + \frac{\gamma}{\gamma+\beta} N_{ox}^+ \tag{38}$$

and

$$\tau_c = \frac{\gamma}{\gamma+\beta}\frac{2}{A\alpha_d^c} \tag{39}$$

is the time of recombination.

Numerical estimates for altitudes ~60 km, using $N_{oe} \simeq 10^{-2}\ cm^{-3}$, $N_{ox}^+ \simeq 1\ cm^{-3}$, $\gamma \simeq 0.2\ s^{-1}$, and $\beta \simeq 1\ s^{-1}$ give $A \simeq 0.2\ cm^{-3}$ and $\tau_c \sim 10^5$ s. For altitudes ~80 km the recombination process is much faster and using $\gamma \simeq 0.02\ s^{-1}$, $\beta \simeq 0.01\ s^{-1}$ and $N_{oe} \simeq 10^2\ cm^{-3}$, $N_{ox}^+ \simeq 10^3\ cm^{-3}$ we have $A \simeq 10^3\ cm^{-3}$ and $\tau_c \simeq 10^2$ s. Since the coefficent of electron-clusters recombination α_d^c is not well known as mentioned above, we can potentially use these results to estimate this quantity by comparison with measured VLF recovery signatures. Thus, the relaxation time of ~100 s observed in the majority of experiments [*Inan et al.*, 1990 and references therein] can be explained by comparatively large values of $\alpha_d^c \geq 10^{-5}\ cm^3\ s^{-1}$.

4. Applications of the Model

In this section, we present some results of the numerical solution of the system of equations (12)-(15) for three different cases. All

parameter values used are the same as those in the work by *Inan et al.* [1988] and references cited therein.

4.1. Production of Secondary Ionization by Precipitating Electron Bursts

We consider processes that take place during the typically short (<1 s) bursts of electron precipitation induced by lightning generated whistlers [*Chang and Inan*, 1985]. For this purpose, we assume a precipitated flux of 10^{-2} erg cm^{-2} s^{-1}, consisting of ~1-MeV electrons; the duration of the electron burst is taken to be τ_s=1 s. We carry out our calculations only up to t=1 s, since we are only interested in this case in the dynamics of the system during the time when the source $I_s(t)$ is applied. The time evolution of the density of different ionospheric constituents is represented in Figures 4*a*, 4*b*, 4*c*4, and 4*d*. From Figure 4*a* we note that the production rate of enhanced ionization decreases with time, as pointed out earlier in connection with equation (30). Determination of the enhanced secondary electron density by simple integration of the production rate (I_s) over time duration τ_s, i.e., as $I_s\tau_s$ (as has been done in previous work [e.g., *Inan et al.* 1988]), would thus in general lead to inaccurate estimates. Figures 4*b* and 4*d* demonstrate the rapid variation (increase) of the number densities of negative ions (N^-) and positive cluster-ions (N_x^+), suggesting that attachment-detachment processes as well as processes of development of clusters dominate over time scales of ~1 s. We further note that on Figures 4*b*, 4*d* the curves corresponding to time t=0.01 s practically coincide with that corresponding to t=0 s. From Figure 4*c*, we note that most of the N^+ formation occurs in ~0.01 s, in contrast to the case of N^- and N_x^+.

We note that while the results illustrated in Figure 4 are for a monoenergetic 1-MeV beam of precipitating electrons, the resulting electron density profile (Figure 4*a*) is quite similar to that computed for whistler-induced electron precipitation at L=2 (see Figure 4 of *Inan et al.* [1988]). Thus, the physical processes that govern the formation of the disturbance illustrated in Figure 4 can be expected to be important for the more realistic cases involving precipitation of electron bursts consisting of particles over a range of energies.

4.2. Relaxation of a Disturbance Produced by 1-MeV Electrons

Results of calculations for $t \geq 0.2$ s modeling the relaxation of an ionospheric disturbance produced by a 0.2-s (i.e., τ_s=0.2 s) burst of precipitating 1-MeV electrons at a flux level of 10^{-2} erg cm^{-2} s^{-1} are shown in Figures 5*a*, 5*b*, 5*c*, and 5*d*. The dynamics of the formation of a quasi-equilibrium distribution of electron density (see discussion in connection with expression (31) in section 3) is evident in the fact that the curves for t=20 s practically coincide with those for t=100 s. The number density of negative ions (Figure 5*b*) increases and reaches a new quasi-equilibrium attachment-detachment state (like electrons). The density of clusters is increased (Figure 5*d*) due to the initially rapid decrease in the disturbed number density of positive ions (Figure 5*c*).

The effects of the electron density disturbance shown in Figure 5*a* on the amplitude and phase of a subionospheric VLF signal can be determined using a quantitative model of VLF propagation such as that described by *Poulsen et al.* [1990]. In general, we can expect the time evolution of the VLF signal amplitude (or phase) to exhibit recovery over a variety of time scales depending on the selective effect on the amplitude versus phase of disturbances at different altitudes. For example, *Poulsen et al.* [1990] showed that, on a single waveguide mode basis, disturbances that consist of enhanced ionization at lower (higher) altitudes tend to lead to larger (smaller) amplitude and smaller (larger) phase changes. Thus, aspects of VLF signal that are sensitive to features at relatively low altitudes might exhibit evidence of the new attachment-detachment quasi-equilibrium, in the form of signal amplitude or phase not recovering to original levels (recovery must occur over ~10^5 s due to recombination with clusters; see numerical estimations above). Features sensitive to higher altitudes would exhibit the usual recovery in ~100 s due to recombination with clusters. Also interesting to note is the relatively rapid change in electron density profile between t=0.2 s and t=1 s. Such initially rapid changes may result in unusual recovery signatures as reported by *Inan et al.* [1988].

4.3. Relaxation of a Disturbance Produced by 300-keV Electrons

We repeat the relaxation calculations done in section 3 for an ionospheric disturbance produced by a 0.2-s burst of precipitating 300-keV electrons at a flux level of 10^{-2} erg cm^{-2} s^{-1}. For this case the penetration of particles and relaxation processes occur at higher altitudes. Results are presented in Figure 6 in the same format as Figure 5. The principal qualitative features of relaxation are the same as for the 1-MeV case. A new attachment-detachment quasi-equilibrium state is still evident from Figure 6*a*. The changes in electron density with respect to the ambient appear to be smaller for the case of Figure 6 than Figure 5; however, we note that the effect of the disturbance on subionospheric VLF signal phase may still be relatively larger or smaller, depending on the alteration of the particular waveguide mode structure and also the change in electrical conductivity (which also depends on the effective electron collision rate) [*Poulsen et al.*, 1992]. We also note from Figure 6*a* the absence of a rapidly recovering layer similar to that in Figure 5*a*, consistent with the experimental results of *Inan et al.* [1988] which showed initially rapid recovery features at low geomagnetic latitudes at which lightning-induced electron precipitation bursts are expected to include ≥1-MeV electrons.

5. Summary and Discussion

A quantitative model of the formation and relaxation of lower ionospheric disturbances caused by lightning induced electron precipitation is proposed which includes four kinds of charged particles, namely electrons, positive ions, negative ions, and positive cluster ions.

Analytical and numerical solutions of the model equations allow us to investigate the processes that are in effect during a short (<1 s) burst of precipitating electrons. Results indicate that at low altitudes (~60 km) a sort of "saturation" effect occurs which limits the number density of electrons. In other words, the number density of electrons is found to depend only weakly on the duration of the electron precipitation burst.

Analytical and numerical investigations of the relaxation of ionospheric disturbances at different altitudes and for different parameters (of precipitating particles) show that, in principle, it may be possible to identify some of the chemical reaction constants of the lower ionosphere ($\gamma, \beta, \alpha_d^c$) on the basis of data on the recovery of VLF signatures. As an example of general trends, we note that the number density of positive cluster ions in wintertime is much less than in summer [*Danilov et al.*, 1981] so that the model predicts in general a slower recovery rate of subionospheric signals in winter than in summer.

In two specific cases involving precipitation of 300-keV and 1-MeV electrons, the model predicts the formation of layers of ionization that represent a different attachment-detachment quasi-equilibrium value from that of the unperturbed ambient. Such new layers may exist for up to $\sim 10^5$ s following electron precipitation bursts and would be exhibited in subionospheric VLF data as apparent signal amplitude and/or phase recoveries to levels other than those prior to the event.

Model calculations for ~1-MeV precipitating electrons also predict the formation and rapid (1 s) disappearance of a secondary electron minilayer that might lead to initially rapid recovery signatures in VLF phase and amplitude as observed at low geomagnetic latitudes [*Inan et al.*, 1988]. Quantitative comparison of experimental data with model predictions may be useful in determining the existence of high energy (1 MeV) precipitating electron bursts and might also allow a determination of the energy flux levels.

While we have applied the model to specific selected cases, it should be noted that the general equations (12)-(15) and the ion pair production rate (11) are generally valid and can be numerically solved at all D region altitudes ($\leq$90 km) and for any energy and flux distribution of precipitating electrons. The model described here can be combined with existing quantitative models of the whistler-induced precipitation process which predict the energy spectrum and temporal signature of the precipitation bursts [*Chang and Inan*, 1985], and the models describing the propagation of VLF waves in the Earth-ionosphere waveguide in the presence of localized disturbances [e.g., *Poulsen et al.*, 1990]. In this sense, the model described here fills in a gap in our theoretical modeling of the processes that lead to subionospheric VLF perturbations observed in association with lightning discharges.

Acknowledgments. We appreciate comments on the text of our colleagues in the STAR Laboratory, especially those of Juan Rodriguez and A. Draganov. We thank Zheng Xu for her expert help with the typesetting of the manuscript. The Stanford component of this work was sponsored by the National Science Foundation under grant NSF-ATM8804273.

The Editor thanks two referees for their assistance in evaluating this paper.

REFERENCES

Chamberlain, J. W., *Physics of the Aurora and Airglow*, Academic, San Diego, Calif., 1961.

Chamberlain, J. W., *Theory of Planetary Atmospheres: An Introduction to Their Physics and Chemistry*, Academic, San Diego, Calif., 1978.

Chang, H. C., and U. S. Inan, Test particle modeling of wave-induced energetic electron precipitation, *J. Geophys. Res.*, *90*, 6409, 1985.

Danilov, A. D., V. K. Semyonov, and A. G. Simonov, A model for the relative ion composition in Physics and Chemistry of the Lower Ionosphere (in Russian), *Ionos. Res.*, *34*, pp. 73-97, Acad. of Sci. of the USSR, Sov. Geophys. Comm., Moscow, 1981.

Dowden, R. L., and C. D. D. Adams, VLF versus MF heating of the lower ionosphere, *J. Geophys. Res.*, *96*, 14,179, 1991.

Gledhill, J. A., The effective recombination coefficient of electrons in the ionosphere between 50 and 150 km, *Radio Sci.*, *21*, 399, 1986.

Goldberg, R. A., J. R. Barcus, L. C. Hale, and S. A. Curtis, Direct observation of magnetospheric electron precipitation stimulated by lightning, *J. Atmos. Terr. Phys.*, *48*, 293, 1986.

Inan, U. S., and D. L. Carpenter, Lightning-induced electron precipitation events observed at $L \sim 2.4$ as phase and amplitude perturbations on subionospheric VLF signals, *J. Geophys. Res.*, *92*, 3293, 1987.

Inan, U. S., W. C. Burgess, T. G. Wolf, D .C. Shafer, and R. E. Orville, Lightning-associated precipitation of MeV electrons from the inner radiation belt, *Geophys. Res. Lett.*, *15*, 172, 1988.

Inan, U. S., M. Walt, H. D. Voss, and W. L. Imhof, Energy spectra and pitch angle distributions of lightning-induced electron precipitation: Analysis of an event observed on the S81-1 (SEEP) satellite, *J. Geophys. Res.*, *94*, 1379, 1989.

Inan, U. S., F. A. Knifsend, and J. Oh, Subionospheric VLF "imaging" of lightning-induced electron precipitation from the magnetosphere, *J. Geophys. Res.*, *95*, 17,217, 1990.

Inan, U. S., T. F. Bell, and J. V. Rodriguez, Heating and ionization of the lower ionosphere by lightning, *Geophys. Res. Lett.*, *18*, 705, 1991.

Ivanov-Holodny, G. S., and G. M. Nikolsky, *Sun and the Ionosphere* (in Russian), Science, Moscow, 1969.

Mitra, A. P., A review of D region processes in non-polar latitudes, *J. Atmos. Terr. Phys.*, *30*, 1065, 1968.

Mitra, A. P., D region in disturbed conditions, including flares and energetic particles, *J. Atmos. Terr. Phys.*, *37*, 895, 1975.

Mitra, A. P., Chemistry of middle atmospheric ionization - A review, *J. Atmos. Terr. Phys.*, *43*, 737, 1981.

Poulsen, W. L., T. F. Bell, and U. S. Inan, 3-D modeling of subionospheric VLF propagation in the presence of localized D region perturbations associated with lightning, *J. Geophys. Res.*, *95*, 2355, 1990.

Poulsen, W. L., U. S. Inan, and T. F. Bell, A multiple-mode three dimensional model of VLF propagation in the Earth-ionosphere waveguide in the presence of licalized D region disturbances, *J. Geophys. Res.*, in press, 1992.

Reagan, J. B., R. E. Meyerott, R. C. Gunton, W. L. Imhof, E. E. Gaines, and T. R. Larsen, Modeling of the ambient and disturbed ionospheric media pertinent to ELF/VLF propagation, in *Proceedings of NATO-AGARD Meeting on Medium, Long, and Very Long Wave Propagation*, Brussels, Belgium, 1981.

Rees, M. H., Auroral ionization and excitation by incident energetic electrons, *Planet. Space Sci.*, *11*, 1209, 1963.

Rishbeth, H., and O. K. Garriott, *Introduction to Ionospheric Physics*, Academic Press, San Diego, Calif., 1969.

Rowe, J. N., A. P. Mitra, A. J. Ferraro, and H. S. Lee, An experimental and theoretical study of the D region, II, A semi-empirical model for mid-latitude D-region, *J. Atmos. Terr. Phys.*, *36*, 755, 1974.

Tolstoy, A., T. J. Rosenbert, U. S. Inan, and D. L. Carpenter, Model predictions of subionospheric VLF signal perturbations resulting from localized, electron precipitation-induced ionization enhancement regions, *J. Geophys. Res.*, *91*, 13, 473, 1986.

Voss, H. D., W. L. Imhof, J. Mobilia, E. E. Gaines, M. Walt, U. S. Inan, R. A. Helliwell, D. L. Carpenter, J. P. Katsufrakis, and H. C. Chang, Lightning induced electron precipitation, *Nature*, *312*, 740, 1984.

Wolf, T. G., and U. S. Inan, Path-dependent properties of subionospheric VLF amplitude and phase perturbations associated with lightning, *J. Geophys. Res.*, *95*, 20,997, 1990.

V. S. Glukhov and V. P. Pasko, Department of Astronomy, Kiev State University, Vladimirskaya 65, Kiev 252017, Ukraine.

U. S. Inan, STAR Laboratory, Department of Electrical Engineering, Stanford University, Stanford, CA 94305.

(Received February 14, 1992;
accepted May 29, 1992.)